JOURNAL OF AIRCRAFT
Vol. 45, No. 5, September–October 2008

Engineering Notes

ENGINEERING NOTES are short manuscripts describing new developments or important results of a preliminary nature. These Notes should not exceed 2500 words (where a figure or table counts as 200 words). Following informal review by the Editors, they may be published within a few months of the date of receipt. Style requirements are the same as for regular contributions (see inside back cover).

Transonic Aeroelastic Analysis of All-Movable Wing with Free Play and Viscous Effects

Jong-Yun Kim,* Kyung-Seok Kim,* and In Lee†
Korea Advanced Institute of Science and Technology, Daejeon 305-701, Republic of Korea
and
Young-Keun Park‡
Agency for Defense Development, Daejeon 305-600, Republic of Korea

DOI: 10.2514/1.37435

Nomenclature

$[C]$	=	damping matrix
C_E	=	entrainment coefficient
C_f	=	skin-friction coefficient
$[C_g]$	=	generalized damping matrix
C_p	=	pressure coefficient
C_τ	=	shear stress coefficient
$\bar{H}$	=	boundary-layer shape factors
H_1	=	Head's boundary-layer shape factor
$[K]$	=	stiffness matrix
K_α	=	linear stiffness at the free-play node
M	=	freestream Mach number
$[M]$	=	mass matrix
$[M_g]$	=	generalized mass matrix
$\{Q\}$	=	generalized aerodynamic forces vector
$\{q\}$	=	generalized modal displacement vector
$\{R\}$	=	restoring force vector including structural nonlinearities
S	=	wing area
s	=	free-play angle at the free-play node
t	=	time, nondimensionalized by U/c_r
U	=	freestream velocity
x, y, z	=	nondimensional physical coordinates in the streamwise, spanwise, and vertical directions, respectively
α_{ip}	=	initial pitch angle at the free-play node
γ	=	specific heat ratio
θ	=	boundary-layer momentum thickness
ρ	=	freestream density
ϕ	=	disturbance velocity potential
$[\psi_b]$	=	modal matrix

Received 7 March 2008; revision received 12 May 2008; accepted for publication 21 May 2008.

*Graduate Research Assistant, Department of Aerospace Engineering, 335 Gwahangno, Yuseong-gu.
†Professor, Ph.D., Department of Aerospace Engineering, 335 Gwahangno, Yuseong-gu. Associate Fellow AIAA.
‡Senior Researcher, Ph.D., The 3rd R&D Center, Yuseong P.O. Box 35-7.

I. Introduction

UNSTABLE aeroelastic problems are critical at aircraft design stages. Particularly, the estimation of stability for aeroelastic problems in the transonic regime is necessary due to the transonic dip. There are many categories of aeroelastic phenomena, which are the interaction between the elastic motions of structures and the resulting aerodynamic forces, and they are grouped according to physical features including flutter, divergence, gust response, buffeting, limit cycle oscillations (LCOs), and others. All aeroelastic phenomena categories should be considered in aircraft design because the structural flexibility resulting from light materials in modern aircraft is more susceptible to aeroelastic phenomena. Among the aforementioned categories, LCO and flutter, which can result in complete structural failure within seconds, are the most dangerous dynamic problems. LCOs are continuous oscillations with a limited amplitude at a flight speed below the critical speed of flutter. The oscillations could continuously affect the fatigue of aircraft structures and, finally, the structures could fail. Real aircraft not only have structural nonlinearities such as friction, free play, and hysteresis, but also aerodynamic nonlinearities such as shock waves. Among the structural nonlinearities, free play is inevitable for the control surfaces of aircraft. The viscous effects with shock waves in the transonic regime are typical aerodynamic nonlinearities; in practice, these nonlinearities lead to LCOs.

For the past few decades, much research on aeroelastic analysis with free play has been conducted. Laurenson and Trn [1] used the describing function method to investigate the aeroelastic responses of a missile control surface with free play and showed that LCOs could be obtained at velocities below the linear flutter boundary. Kim and Lee [2] studied a 2-D flexible airfoil with free play in which the airfoil was modeled using beam elements. Bae et al. [3] investigated the nonlinear aeroelastic characteristics of a wing with free play using frequency and time domain analyses. The frequency domain analyses were performed using the describing function and velocity-damping (v-g) methods. The time domain analyses were accomplished with the time integration of unsteady aerodynamic forces approximated by a rational function. For the inclusion of aerodynamic nonlinearities, many aerodynamic or aeroelastic analyses using the computational fluid dynamics (CFD) technique have been performed in the transonic regime. Specifically, an aeroelastic study using an efficient unsteady aerodynamic analysis tool such as the transonic small disturbance (TSD) equation, which is widely recognized as one of the most efficient theories among the conventional CFD-based approaches, can have strong computational advantages in many different types of parametric studies [4]. Batina [5] formulated a time-accurate approximate factorization (AF) algorithm as a solution for the three-dimensional unsteady TSD equation. Moreover, Batina et al. [6] laid the cornerstone of practical aeroelastic analysis for three-dimensional aircraft models using transonic unsteady aerodynamics, and the aeroelastic code was developed for application in practical aircraft configurations. Kim and Lee [7] performed an aerodynamic analysis of a wing in the transonic region using the TSD code, which was also applied in the present study. Kousen and Bendiksen [8] studied the aeroelastic characteristics of 2-D airfoil models in the transonic regime using the

Euler equations and showed that LCOs could occur due to the nonlinear aerodynamic forces induced by the shock. They later extended the analysis to include free-play nonlinearities and showed that the flutter velocity drops [9]. To improve the accuracy of the efficient TSD equation, Howlett [10] and Edwards [11] applied the coupled TSD and boundary-layer equations to deal with viscous flows in the boundary layer. Zhang et al. [12] applied the Euler equations coupled to the same viscous formulations.

In the present study, an aeroelastic analysis considering structural nonlinearities due to free play and aerodynamic nonlinearities due to shock waves and viscous effects of the boundary layer is performed. The fictitious mass (FM) method is used to apply a modal approach for an efficient structural analysis of the nonlinear structural models. The TSD equation is used to calculate the unsteady aerodynamic forces in the transonic regime. By coupling the viscous equations to the TSD equation, the aerodynamic results are improved. The nonlinear aeroelastic responses are computed using the coupled time integration method (CTIM) in the time domain. Finally, for an all-movable wing with free play, the nonlinear aeroelastic responses with viscous effects in a transonic Mach number are compared with those without viscous effects.

II. Theoretical Background

A. Unsteady Transonic Small Disturbance Equation and Viscous Equations

Although Navier–Stokes equations are the most accurate aerodynamic equations, many flow features depend on a precise evaluation of the viscous and turbulent terms. If the thickness value of a wing section is small and there is no boundary-layer separation, the viscosity has little effect on the flowfields. If the viscous terms are removed from the Navier–Stokes equations, the equations become the Euler equations. Furthermore, if the flow around the aircraft wing is irrotational and the perturbation is small, the TSD theory can be applied. A three-dimensional unsteady TSD equation can be written in a conservation law form as [5]

$$\frac{\partial f_0}{\partial t}+\frac{\partial f_1}{\partial x}+\frac{\partial f_2}{\partial y}+\frac{\partial f_3}{\partial z}=0 \tag{1}$$

where

$$f_0=-A\phi_t-B\phi_x,\qquad f_1=E\phi_x+F\phi_x^2+G\phi_y^2,$$
$$f_2=\phi_y(1+H\phi_x),\qquad f_3=\phi_z$$

These equations are given in a physical coordinate system (x, y, z, t), and the subscripts x, y, and z denote the derivative of the streamwise, spanwise, and vertical directions, respectively. t and x, y, and z are nondimensionalized by U/c_r and c_r, respectively. ϕ represents the disturbance velocity potential. The coefficients A, B, and E, are determined by the freestream Mach number M. The other coefficients, F, G, and H, are related to both the freestream Mach number and the specific heat ratio, γ, and the coefficients can be chosen depending on the assumptions used when deriving the TSD equation. All coefficients are defined in [13].

For more accurate results in the TSD equation for the transonic regime with strong shock waves, the viscous effects should be considered. The effect of a turbulent viscous boundary layer for attached flows is modeled in a quasi-steady manner by Green's lag-entrainment equations. The boundary-layer equations for attached flows can be expressed as [10]

$$\frac{\mathrm{d}\theta}{\mathrm{d}x}=\tfrac{1}{2}C_f-(H+2-M_e^2)\theta\phi_{xx} \tag{2}$$

$$\theta\frac{\mathrm{d}\bar{H}}{\mathrm{d}x}=\left(C_E-\frac{1}{2}H_1C_f\right)\frac{\mathrm{d}\bar{H}}{\mathrm{d}H_1}+H_1(H+1)\frac{\mathrm{d}\bar{H}}{\mathrm{d}H_1}\theta\phi_{xx} \tag{3}$$

$$\theta\frac{\mathrm{d}C_E}{\mathrm{d}x}=F\left\{\frac{2.8}{H+H_1}[(C_\tau)_{EQO}-\lambda C_\tau^{1/2}]+\left(\frac{\theta}{U_e}\frac{\mathrm{d}U_e}{\mathrm{d}x}\right)_{EQ}\right\}$$
$$-F\left(1+0.075M_e^2\frac{1+\frac{\gamma-1}{2}rM_e^2}{1+0.1M_e^2}\right)\theta\phi_{xx} \tag{4}$$

where the subscript e refers to the quantities at the boundary-layer edge.

For mild separation flows, the boundary-layer equations are written in inverse form. In an inverse boundary-layer calculation, the pressure or velocity at the boundary-layer edge is solved from a given distribution of boundary-layer displacement thickness as represented by a perturbation mass flow parameter, $\bar{m}=\rho_eU_e\delta^*$ [12]:

$$\frac{H\theta}{\bar{m}}\frac{\mathrm{d}\bar{m}}{\mathrm{d}x}=H\frac{\mathrm{d}\theta}{\mathrm{d}x}+R_1\theta\frac{\mathrm{d}\bar{H}}{\mathrm{d}x}+[(H+1)R_3+H(1-M_e^2)]\frac{\theta}{U_e}\frac{\mathrm{d}U_e}{\mathrm{d}x} \tag{5}$$

$$C_E=H_1\frac{\mathrm{d}\theta}{\mathrm{d}x}+H_1(1-M_e^2)\frac{\theta}{U_e}\frac{\mathrm{d}U_e}{\mathrm{d}x}+\theta\frac{\mathrm{d}H_1}{\mathrm{d}\bar{H}}\frac{\mathrm{d}\bar{H}}{\mathrm{d}x} \tag{6}$$

$$\frac{C_f}{2}=\frac{\mathrm{d}\theta}{\mathrm{d}x}+(H+2-M_e^2)\frac{\theta}{U_e}\frac{\mathrm{d}U_e}{\mathrm{d}x} \tag{7}$$

$$\theta\frac{\mathrm{d}C_E}{\mathrm{d}x}=F\left\{\frac{2.8}{H+H_1}[(C_\tau)_{EQO}^{1/2}-\lambda C_\tau^{1/2}]+\left(\frac{\theta}{U_e}\frac{\mathrm{d}U_e}{\mathrm{d}x}\right)_{EQ}\right.$$
$$\left.-\left[1+0.075M_e^2\frac{R_1}{1+0.1M_e^2}\right]\frac{\theta}{U_e}\frac{\mathrm{d}U_e}{\mathrm{d}x}\right\} \tag{8}$$

Various parameters in the viscous equations of attached and separated flows are defined in [10–12]. Numerical integration of the viscous equations is performed using a fourth-order Runge–Kutta method.

B. Aeroelastic Equation of Motion

The aeroelastic equation of motion with structural nonlinearities can be written as [14]

$$[M]\{\ddot{u}\}+[C]\{\dot{u}\}+\{R(u)\}=\{F(t,u,\dot{u})\} \tag{9}$$

where $\{F\}$ is the external aerodynamic force vector, which is a time-dependent function of the displacement and velocity. $\{R(u)\}$ is the elastic restoring force vector including structural nonlinearities and can be written as

$$\{R(u)\}=[K]\{u\}+\{f(\alpha)\} \tag{10}$$

where $\{f(\alpha)\}$ is the restoring force vector resulting from the structural nonlinear factors and is given by

$$f(\alpha)=\begin{cases}K_\alpha(\alpha-s), & \alpha>s\\ 0, & -s\le\alpha\le s\\ K_\alpha(\alpha+s), & \alpha<-s\end{cases} \tag{11}$$

Usually, aeroelastic analysis is conducted using a modal approach method with a limited number of low-frequency modes to reduce the computational effort required. However, for wing models with free play, the normal modal approach cannot be used due to the stiffness variation with the displacement. Karpel and Wieseman [15] proposed the FM method, and Lee and Kim [16] described the application of the FM method to a three-dimensional wing model with free play. After the modal matrix, $[\psi_b]$, is obtained from the FM model, the displacement vector can be expressed as

$$\{u(t)\}=[\psi_b]\{q(t)\} \tag{12}$$

The final matrix form of the aeroelastic equation of motion with free play in the generalized coordinates is written in matrix form as follows:

$$[M_g]\{\ddot{q}\} + [C_g]\{\dot{q}\} + \{R_g(u)\} = \{Q\} \tag{13}$$

where $\{R_g(u)\}$ is the generalized restoring force vector defined as

$$\{R_g(u)\} = [\psi_b]^T[K][\psi_b]\{q\} - [\psi_b]^T\{f(\alpha)\} \tag{14}$$

$$\{Q\} = [\psi_b]^T \frac{1}{2}\rho U^2 \int_s \Delta C_p \, \mathrm{d}S \tag{15}$$

where ρ is the freestream density, U is the velocity of the freestream, S is the area of the lifting surfaces, and ΔC_p is the difference of the pressure coefficients between the upper and lower lifting surfaces.

III. Numerical Results and Discussion

The aerodynamic analysis is performed using the coupled TSD and boundary-layer equations. Figure 1 shows a comparison of the steady pressure coefficients for the NACA 0012 airfoil model. A NACA 0012 airfoil, by definition, has 12% thickness. The freestream Mach number, M, is 0.775, and the angle of attack, α_0, is 2.05 deg. For the viscous case, the Reynolds number, Re, is 1.0×10^7. Although the airfoil is symmetric, the shock wave only exists on the upper surface due to the nonzero angle of attack. The results of the inviscid and viscous TSD codes are compared with the experimental data in [17]. The thin and thick lines indicate the steady coefficients of the inviscid and viscous TSD codes, respectively. By coupling the TSD solution with the viscous effects, the shock wave position of the viscous TSD code is closer to the experimental data than that of the inviscid TSD code, and the results of the viscous TSD code agree well with the experimental data downstream of the shock wave.

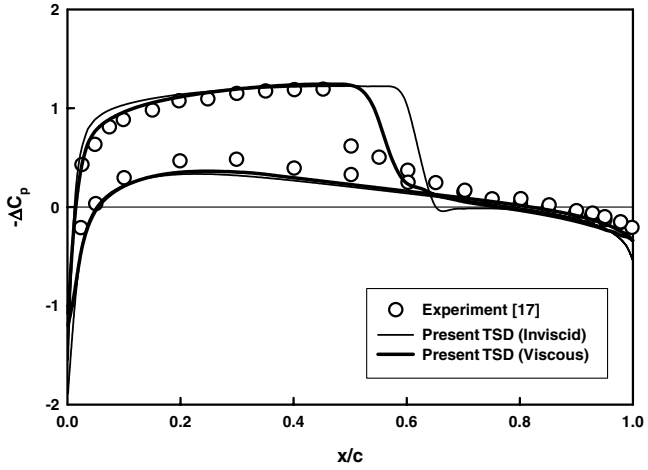

Fig. 1 Comparison of the steady pressure coefficients for the NACA 0012 airfoil model at $M = 0.775$, $\alpha_0 = 2.05$ deg, and $Re = 1.0 \times 10^7$.

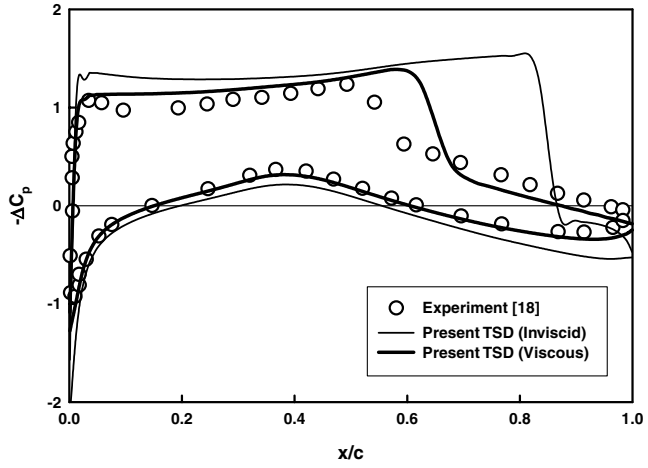

Fig. 2 Comparison of the steady pressure coefficients for the RAE 2822 airfoil model at $M = 0.750$, $\alpha_0 = 2.81$ deg, and $Re = 6.2 \times 10^6$.

For thick airfoil models, such as the RAE 2822 airfoil, the inviscid TSD code has often produced quite different results from the experimental data, as shown in Fig. 2. Figure 2 shows a comparison of the steady pressure coefficients for the RAE 2822 airfoil model, which is asymmetric, at $M = 0.750$ and $\alpha_0 = 2.81$ deg. The viscous aerodynamic analysis is performed at $Re = 6.2 \times 10^6$. The thick line denotes the steady coefficient from the TSD code with viscous effects. The experimental data of the RAE 2822 airfoil model are presented in [18]. The results from the viscous TSD code agree well with the experimental data. The results of the NACA 0012 and RAE 2822 airfoils ensure that the viscous analysis has more accurate aerodynamic results than the inviscid analysis in the transonic regime.

For the LCO analysis, an all-movable wing model is considered in this study, as shown in Fig. 3a. The model is similar to the control fin of missiles. The wing model has an aspect ratio of 2.564, a taper ratio of 0.5, and a leading-edge sweepback angle of 27.47 deg. The structural thickness of the wing is 0.002 m, and the root chord length is 0.156 m. For the wing section, a 4% biconvex airfoil is used. For the motions of the all-movable wing, the pitching axis is located at half-root chord and has a linear stiffness, K_α, of 100 Nm/rad. In the present study, symmetric free play around the pitching axis is considered for structural nonlinearities, as indicated in Fig. 3b.

Six elastic modes are used in the aeroelastic analysis of the wing model. For an efficient modal approach including the stiffness variation due to free play, the FM method is applied to the all-movable wing model. The elastic modes obtained from the FM method are appropriate for the modal transformation of a structure with a concentrated nonlinearity.

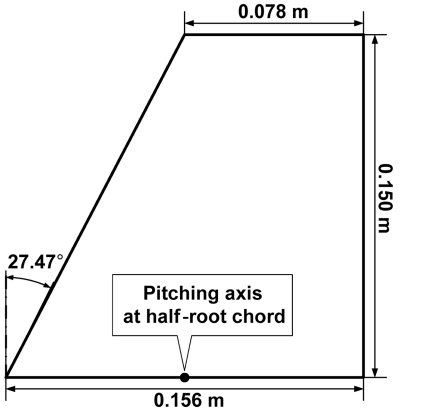

a) Configuration of the all-movable wing model

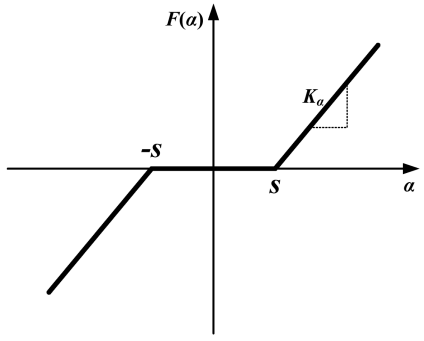

b) Symmetric free play

Fig. 3 Configuration of the all-movable wing model and restoring moment for pitch angle, α, with symmetric free play.

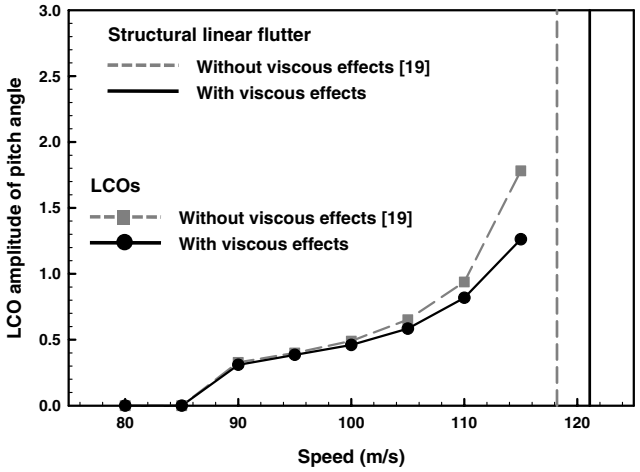

a) $s = 0.1$ deg

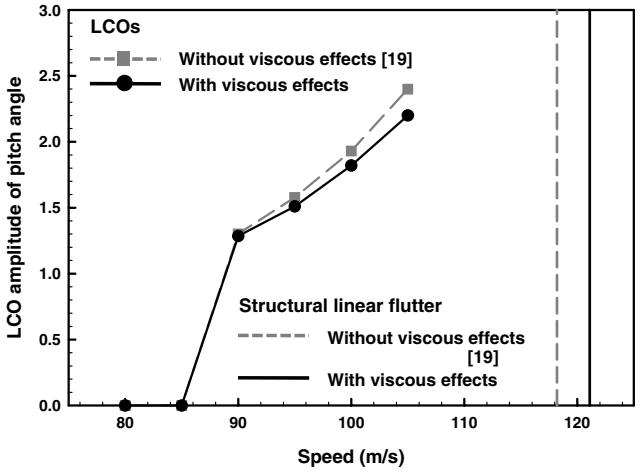

b) $s = 0.4$ deg

Fig. 4 Comparison of the LCO amplitudes at $M = 0.90$ and $\alpha_{ip} = 1.6$ deg.

Figure 4 shows the changes of the LCO amplitudes with increasing flight speed for the free-play angles, s, of 0.1 and 0.4 deg at the pitching axis. The figure also shows a comparison of the LCO amplitudes both with and without viscous effects. The freestream Mach number, M, is 0.90, and the initial pitch angle is 1.6 deg. The Reynolds number is 2.0×10^6 for the viscous case. The linear flutter speed and results of the LCO amplitudes from the inviscid TSD code are presented in [19]. The linear flutter speed from the viscous TSD code is 121.0 m/s, whereas that of the inviscid TSD code is 118 m/s. The LCO onset speeds from the viscous TSD code are almost identical to those from the inviscid TSD code for both free-play angles of 0.1 and 0.4 deg. As the size of the free play increases, the LCO amplitude increases for both the inviscid and viscous cases. For both free-play angles of 0.1 and 0.4 deg, however, the LCO amplitudes obtained from the viscous TSD code are smaller than those from the inviscid TSD code.

Figure 5 shows the pitch angles at the pitch axis with and without viscous effects at a speed, V, of 115 m/s and a free-play angle, s, of 0.1 deg. Figure 6 shows a comparison of distributions of the pressure coefficient differences with and without viscous effects at 45% semispan of the all-movable wing model. The freestream Mach number, M, is 0.90, the pitch angle is 1.6 deg, and the Reynolds number is 2.0×10^6. Although the aerodynamic results of the case without viscous effects includes the weak shock at half of the chord, the shock disappears in the case with viscous effects. Moreover, the sign of the pressure differences of the case without viscous effects is converted around the pitch axis. The aerodynamic characteristics affect the aspect of transition before the appearance of the LCO and the LCO amplitudes, as shown in Fig. 5.

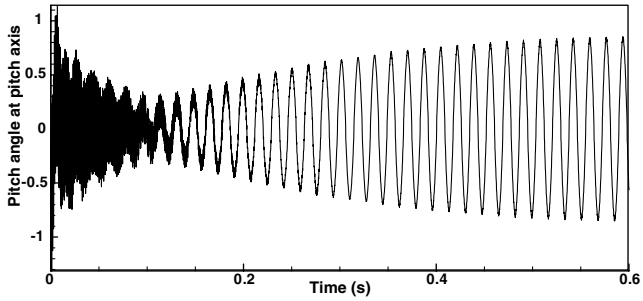

a) Without viscous effects

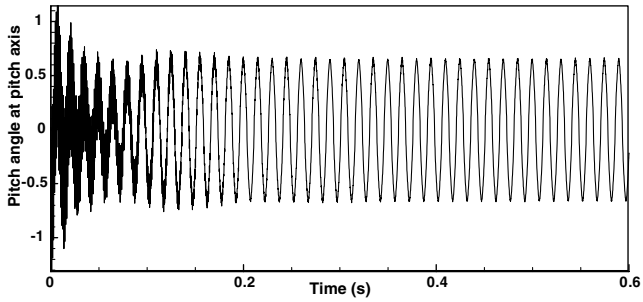

b) With viscous effects

Fig. 5 Pitch angles at the pitch axis with and without viscous effects at $V = 115$ m/s and $s = 0.1$ deg ($M = 0.90$ and $\alpha_{ip} = 1.6$ deg).

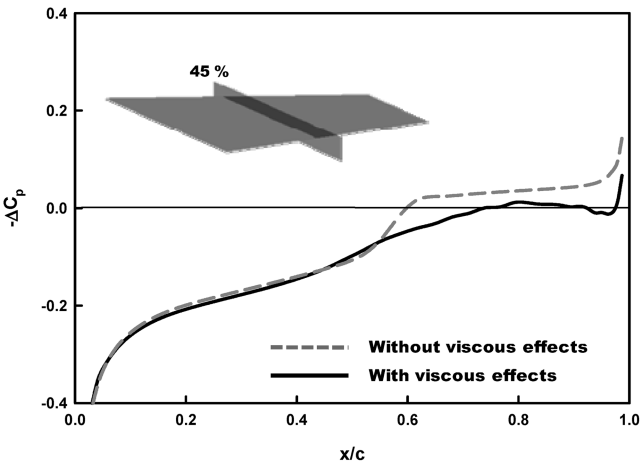

Fig. 6 Comparison of distributions of the pressure coefficient differences for the all-movable wing model at $M = 0.90$, $\alpha_0 = 1.6$ deg, and $Re = 2.0 \times 10^6$.

IV. Conclusions

In this study, an aeroelastic analysis considering the structural nonlinearities due to free play and the aerodynamic nonlinearities due to shock waves and viscous effects was performed. For the development of an efficient modal approach of a structure with free play, the FM method was used, and the TSD equation was applied to calculate the unsteady aerodynamic forces in the transonic region. Moreover, the viscous effects of the boundary layer were coupled with the TSD equation for more accurate aerodynamic results. Finally, for an all-movable wing with free play, the characteristics of the LCOs with viscous effects, in a transonic Mach number, were compared with those without viscous effects. The inclusion of viscous effects caused the linear flutter velocity to increase and the LCO amplitudes to decrease when compared with the corresponding results without viscous effect.

Acknowledgments

This work was supported by the second stage of the Brain Korea 21 Project in 2008 and the Defense Acquisition Program

Administration and Agency for Defense Development under contract UD070041AD.

References

[1] Laurenson, R. M., and Trn, R. M., "Flutter Analysis of Missile Control Surfaces Containing Structural Nonlinearities," *AIAA Journal*, Vol. 18, No. 10, 1980, pp. 1245–1251. doi:10.2514/3.50876

[2] Kim, S.-H., and Lee, I., "Aeroelastic Analysis of a Flexible Airfoil with a Freeplay Nonlinearity," *Journal of Sound and Vibration*, Vol. 193, No. 4, 1996, pp. 823–846. doi:10.1006/jsvi.1996.0317

[3] Bae, J.-S., Yang, S.-M., and Lee, I., "Linear and Nonlinear Aeroelastic Analysis of Fighter-Type Wing with Control Surface," *Journal of Aircraft*, Vol. 39, No. 4, 2002, pp. 697–708.

[4] Kim, D.-H., and Lee, I., "CFD-Based Matched-Point Transonic and Supersonic Flutter Computations Using a Modified TSD Equation," *Computational Fluid Dynamics Journal*, Vol. 11, No. 1, 2002, pp. 35–49.

[5] Batina, J. T., "Efficient Algorithm for Solution of the Unsteady Transonic Small-Disturbance Equation," *Journal of Aircraft*, Vol. 25, No. 7, 1988, pp. 598–605. doi:10.2514/3.45629

[6] Batina, J. T., Seidel, D. A., Bland, S. R., and Bennett, R. M., "Unsteady Transonic Flow Calculations for Realistic Aircraft Configurations," *Journal of Aircraft*, Vol. 26, No. 1, 1989, pp. 21–28. doi:10.2514/3.45718

[7] Kim, D.-H., and Lee, I., "Transonic and Low-Supersonic Aerodynamic Analysis of a Wing with Underpylon/Store," *Journal of Aircraft*, Vol. 37, No. 1, 2000, pp. 189–192.

[8] Kousen, K. A., and Bendiksen, O. O., "Nonlinear Aspects of the Transonic Aeroelastic Stability Problem," AIAA Paper 88-2306, 1988.

[9] Kousen, K. A., and Bendiksen, O. O., "Limit Cycle Phenomena in Computational Transonic Aeroelasticity," *Journal of Aircraft*, Vol. 31, No. 6, 1994, pp. 1257–1263. doi:10.2514/3.46644

[10] Howlett, J. T., "Calculation of Unsteady Transonic Flows with Mild Separation by Viscous-Inviscid Interaction," NASA TP-3197, 1992.

[11] Edwards, J. W., "Transonic Shock Oscillations and Wing Flutter Calculated with an Interactive Boundary Layer Coupling Method," NASA TM-110284, 1996.

[12] Zhang, Z., Liu, F., and Schuster, D. M., "Calculations of Unsteady Flow and Flutter by an Euler and Integral Boundary-Layer Method on Cartesian Grids," AIAA Paper 2004-5203, 2004.

[13] Kim, J.-Y., Kwon, H.-J., Kim, K.-S., Lee, I., and Han, J.-H., "Numerical Investigation on the Aeroelastic Instability of a Complete Aircraft Model," *Japan Society of Mechanical Engineers International Journal. Series B. Fluids and Thermal Engineering*, Vol. 48, No. 2, 2005, pp. 212–217 doi :10.1299/jsmeb.48.212.

[14] Park, Y.-K., Yoo, J.-H., and Lee, I., "Effects of Angle-of-Attack on the Aeroelastic Characteristics of a Wing with Freeplay," *Journal of Spacecraft and Rockets*, Vol. 43, No. 6, 2006, pp. 1419–1422. doi:10.2514/1.21368

[15] Karpel, M., and Wieseman, C. D., "Modal Coordinates for Aeroelastic Analysis with Large Local Structural Variation," *Journal of Aircraft*, Vol. 31, No. 2, 1994, pp. 396–400. doi:10.2514/3.46499

[16] Lee, I., and Kim, S.-H., "Aeroelastic Analysis of a Flexible Control Surface with Structural Nonlinearity," *Journal of Aircraft*, Vol. 32, No. 4, 1995, pp. 868–874. doi:10.2514/3.46803

[17] Edwards, J. W., "Transonic Shock Oscillations Calculated with a New Interactive Boundary Layer Coupling Method," AIAA Paper 1993-777, 1993.

[18] Fenno, C. C., Jr., Newman, P. A., and Hassan, A., "Unsteady Viscous Inviscid Procedure for Transonic Airfoils Using Cartesian Grids," *Journal of Aircraft*, Vol. 26, No. 8, 1989, pp. 723–730. doi:10.2514/3.45831

[19] Park, Y.-K., Yoo, J.-H., and Lee, I., "Nonlinear Aeroelastic Analysis of Control with Freeplay in Transonic Region," *AIAA Journal*, Vol. 45, No. 5, 2007, pp. 1142–1145. doi:10.2514/1.14068